A new mouse mutant for the LDL receptor identified using ENU mutagenesis

Karen L. Svenson,[2,*] Nadav Ahituv,[1,†] Rebecca S. Durgin,[*] Holly Savage,[*] Phyllis A. Magnani,[*] Oded Foreman,[*] Beverly Paigen,[*] and Luanne L. Peters[*]

The Jackson Laboratory,[*] Bar Harbor, ME 04609; and Genomics Division,[†] Lawrence Berkeley National Laboratory, Berkeley, CA 94720

Abstract In an effort to discover new mouse models of cardiovascular disease using *N*-ethyl-*N*-nitrosourea (ENU) mutagenesis followed by high-throughput phenotyping, we have identified a new mouse mutation, C699Y, in the LDL receptor (*Ldlr*), named wicked high cholesterol (WHC). When WHC was compared with the widely used *Ldlr* knockout (KO) mouse, notable phenotypic differences between strains were observed, such as accelerated atherosclerotic lesion formation and reduced hepatosteatosis in the ENU mutant after a short exposure to an atherogenic diet. This loss-of-function mouse model carries a single base mutation in the *Ldlr* gene on an otherwise pure C57BL/6J (B6) genetic background, making it a useful new tool for understanding the pathophysiology of atherosclerosis and for evaluating additional genetic modifiers regulating hyperlipidemia and atherogenesis. Further investigation of genomic differences between the ENU mutant and KO strains may reveal previously unappreciated sequence functionality.—Svenson, K. L., N. Ahituv, R. S. Durgin, H. Savage, P. A. Magnani, O. Foreman, B. Paigen, and L. L. Peters. **A new mouse mutant for the LDL receptor identified using ENU mutagenesis. *J. Lipid Res.* 2008.** 49: **2452–2462.**

Supplementary key words *N*-ethyl-*N*-nitrosourea • atherosclerosis • hyperlipidemia • high-throughput phenotyping

The incidence and progression of atherosclerosis remains a challenge for public health intervention and medical research strategies. Mouse models have been of great utility in meeting this challenge and have enabled systematic evaluation of genetic and environmental influences on the pathogenesis of this disease. Lipoproteins and their receptors play crucial roles in cholesterol homeostasis and, when functionally impaired, can accelerate atherogenesis. Mice with targeted mutations resulting in loss of function and those engineered for overexpression of apolipoproteins, their receptors, and key enzymes in lipid metabolism have been used extensively to investigate the complex etiology of atherosclerosis and to develop effective approaches to treatment (1–6). In addition to genetically engineered mouse models, chemical mutagenesis using *N*-ethyl-*N*-nitrosourea (ENU), which causes primarily single-nucleotide mutations, has produced numerous new mouse models for studying human disease. Many of these mutants carry a novel functional mutation in a known gene (7–11). For known genes, having multiple models with a variety of unique mutations allows a survey of phenotypic differences and functional annotation of genes and their products. Causative mutations in numerous ENU mutants identified from large-scale mutagenesis programs worldwide, collectively representing a broad spectrum of disease-related phenotypes, have yet to be identified, and still hold promise of revealing novel genes.

Here we describe the identification and initial characterization of a new mouse model of high cholesterol and atherosclerosis generated using ENU mutagenesis and high-throughput phenotyping. Candidate gene sequencing identified a point mutation in the LDL receptor (*Ldlr*) gene. Comparison of this mutant with the well-characterized *Ldlr* knockout (KO) mouse model reveals certain phenotypic differences and supports it as a new tool for the study of familial hypercholesterolemia (FH) and atherosclerosis.

METHODS

Mice and husbandry

Nonmutagenized C57BL/6J (B6) mice were obtained from The Jackson Laboratory (Bar Harbor, ME). Mice were generated as part of a large-scale mutagenesis effort using high-throughput phenotyping to identify new mouse models of complex heart,

This work was supported by National Heart, Lung, and Blood Institute programs for genomic applications, Grant HL-66611.

Manuscript received 6 June 2008 and in revised form 11 July 2008.

Published, JLR Papers in Press, July 15, 2008.
DOI 10.1194/jlr.M800303-JLR200

Abbreviations: *Apoe*, apolipoprotein E; ATH, atherogenic; ENU, *N*-ethyl-*N*-nitrosourea; FH, familial hypercholesterolemia; G3, three-generation; KO, knockout; *Ldlr*, LDL receptor; WHC, wicked high cholesterol.

[1] Present address: Department of Biopharmaceutical Sciences and Institute for Human Genetics, University of California San Fransisco, San Francisco, CA 94143.

[2] To whom correspondence should be addressed.
e-mail: ksven@jax.org

lung, blood, and sleep disorders. Detailed protocols for generating and phenotyping these ENU cohorts have been described elsewhere (12) and are also available from http://pga.jax.org. Males of inbred mouse strain B6 were treated with ENU in three consecutive weekly doses of 80 mg/kg/body weight, using a previously developed protocol (13, 14). A three-generation (G3) mating scheme obtained both dominant and recessive mutations among the progeny. Apolipoprotein E (*Apoe*) and *Ldlr* KO mice used were Jackson Laboratory stock numbers 2052 and 2207, respectively (http://jaxmice.jax.org/index.html).

Mice were housed in a specific-pathogen-free facility and maintained on a 12 h:12 h light:dark cycle (lights on at 6:00 AM). Mice were housed in pressurized, individually ventilated duplex cages (Maxi-Miser PIV; Thoren Caging Systems, Hazelton, PA) with shaved pine bedding (Crobb Box, Ellsworth, ME) and had free access to acidified water and food, unless otherwise indicated as described below. The Animal Care and Use Committee at The Jackson Laboratory approved all procedures, and research was conducted in conformity with the Public Health Service Policy on Humane Care and Use of Laboratory Animals.

Diets and phenotyping

Each G3 animal was subjected to a 7 week battery of tests starting at 6 weeks of age, while consuming standard rodent chow containing 6% fat by weight (LabDiet 5K52; LabDiet, Scott Distributing, Hudson, NH). Only details of the phenotyping protocol relevant to the identification of the mutant featured in this report are described here. At 8 weeks of age, animals were food deprived for 4 h in the morning, and blood was collected via the retro-orbital sinus through heparin-coated capillary tubes into 1.5 ml Eppendorf tubes containing heparin. Plasma was separated by centrifugation (14,000 rpm for 10 min) and analyzed to determine baseline values of total cholesterol, HDL cholesterol, and triglycerides using a Beckman Coulter Synchron CX®5 Delta autoanalyzer. After blood collection, mice were placed in a clean cage and given an atherogenic (ATH) diet containing (by weight) 15% dairy fat (30% caloric content), 50% sucrose, 1% cholesterol, and 0.5% cholic acid (15). Mice consumed this diet for 5 weeks, at which time another blood sample was collected to assess the effect of the ATH diet. After blood was collected, mice were returned to the standard chow diet to complete the phenotyping protocol. Phenotypic deviants for plasma lipids were identified based on a value exceeding 3.0 standard deviation units from the nonmutagenized B6 control group (n = 15) for each sex and each diet condition.

For assessment of atherosclerotic lesion development, female and male wicked high cholesterol (WHC) mice were provided with three different diets: the standard chow diet; a Western diet containing 21% fat (by weight), 34% sucrose, 0.15% cholesterol, and no cholic acid; and the ATH diet described above. For comparison, *Ldlr* KO mice were fed the chow and ATH diets. Baseline lipids were measured at 8 weeks of age, after which mice were fed a test diet for 5 weeks. Plasma lipids were measured at the end of the diet period, when mice were 13 weeks old. Mice were then fed chow until necropsy at 16–18 weeks of age. Hearts were harvested for qualitative or quantitative histological analysis. Livers were harvested for qualitative analysis.

Heritability testing, colony development, and genetic mapping

To test for heritability of the high-cholesterol trait, phenotypic-deviant G3 females were mated to nonmutagenized B6 males, and the progeny, generation N3F1, were intercrossed without phenotyping. The mode of inheritance (recessive or dominant) was assessed by phenotyping additional N3F1 progeny. Progeny consumed chow from weaning until 8 weeks of age and were then fed the ATH diet for 5 weeks, until age 13 weeks. Affected animals were identified based on 13 week total plasma cholesterol using the same criteria used to identify G3 phenotypic deviants. Affected mice were mated to each other to establish a homozygous colony. Prior to identification of the ENU mutation, homozygosity was presumed for animals with total plasma cholesterol values greater than 1,000 mg/dl after ATH diet feeding. Once a genotype assay was developed, animals were routinely genotyped without completing the 5 week ATH diet protocol. Presumed homozygotes were confirmed by PCR, as described below.

To map the trait, one affected male from the N3F3 generation was bred to DBA2/J (D2) females and F1 progeny were interbred to produce 100 F2 intercross individuals, which were phenotyped using the 5 week ATH diet protocol. DNA was prepared from tails of 17 affected and 17 unaffected F2 animals and used for genotyping with simple sequence length polymorphism DNA markers at an average genome density of 15 cM. Selective pooling of DNA from affected and unaffected F2 animals (16) was used to identify suggestive loci, namely those that are enriched for the B6 allele in the affected pool. Individual samples were amplified with additional markers adjacent to suggestive loci to further evaluate linkage and identify a single best candidate locus.

TABLE 1. LDL receptor (*Ldlr*) primers used for mutation detection

Exon	Forward Primer	Reverse Primer
1	gattcgcagccgagacacc	tttctcgaccaaaaataaaacca
2	tgggtacatttgtcacctctgt	aggttcttctacaaccaccaaca
3	atggacctggtctcaccaaat	cacacccaaggggctgag
4	gaataggctggtgtaagccatag	gggcagtctggttattgctaag
5	tctaactgcaattaagcagaacg	gggaacagcagtaccctaacttt
6	agtgtaatcttaccgcgagcag	acagccccacagtgactacac
7	aagtgttttgcgaaggcagt	tcactgggtggctgaatgt
8	atcctttagccactggaggatac	agatatgggtgaaggcaggtc
9	gcttactagagaaatgggttcca	cagaagaaaggggtcacaataga
10	ctgaccccaggctctattgt	atccaccgtctcccctgag
11	tgtggttccaaactgagaactatt	cctattctcaactatgtactttgtcct
12	ctggcatgttttgaaactttctg	agctgtaattccaatacttctttctaa
13	gaggtggacagtggtgtgtg	cagagtcaagaaaaatggctgac
14	cgcttcctgtacccaataataaa	gacagctggacatctggtca
15	cgttccacccagagcagag	ccacaaatacatcacatcactgt
16	cctgtcccctctctgatgtct	atccctcaggcaggggtatt
17	cattcaaaacatatcgctgtcac	ctctccttccactccacctaact

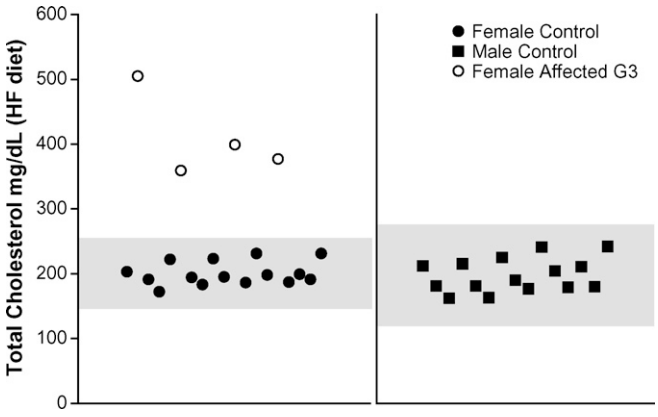

Fig. 1. Identification of three-generation phenotypic deviants based on comparison of total plasma cholesterol values to B6 controls after consuming the atherogenic (ATH) diet for 5 weeks. Shaded areas show 3.0 standard deviation range from average control values.

TABLE 2. Identification of phenotypic deviants with elevated plasma total cholesterol after feeding an atherogenic (ATH) diet

	CHOL Chow	CHOL ATH	HDL Chow	HDL ATH	TG Chow	TG ATH
			mg/dl			
B6 F controls	69 (2)	200 (5)	54 (4)	64 (3)	84 (4)	44 (3)
G3 35363 F	94	359	63	46	103	55
G3 35364 F	89	399	49	41	135	57
G3 35367 F	88	377	55	49	85	51
G3 32776 F	87	505	63	54	94	50

Plasma was analyzed from 4 h-fasted animals before (Chow) and after (ATH) consuming the ATH diet for 5 weeks. B6, C57BL/6J controls (n = 15); G3, original *N*-ethyl-*N*-nitrosourea (ENU) phenotypic deviant; F, female; CHOL, total cholesterol; HDL, HDL cholesterol; TG, triglycerides. Control values are average and (standard error) for each parameter.

Sequencing and PCR assay for genotyping mutants

Primers flanking mouse *Ldlr* splice sites (**Table 1**) were designed using Primer3 (http://frodo.wi.mit.edu/) to give a maximum product size of 500 bp and a minimum of 40 bp into the intron, so that the splice sites were included. Bidirectional sequencing was carried out using the BigDye Terminator v3.1 Cycle Sequencing Kit (Applied Biosystems, Foster City, CA) and run on a 3730xl DNA Analyzer (Applied Biosystems). Once the mutation was discovered, a genotyping assay was developed using Exon 14 primers (Table 1). The 325 bp amplification product was digested for 2 h with restriction endonuclease *Bgl*I. Wild-type (B6) animals produce a 256 bp and a 69 bp product, and animals homozygous for the mutation produce a single 325 bp product.

Histology

Animals were euthanized by CO_2 asphyxiation for collection of tissues for histological analysis. For qualitative assessment, tissues were fixed in Bouin's fixative and embedded in paraffin, and 3–5 μm sections were prepared and stained with hematoxylin and eosin (H and E). Further analysis was done on liver sections stained with periodic acid-Schiff and on aortic sections stained with Masson's trichrome. For quantitative assessment of aortic atherosclerosis, hearts were dissected and sections were stained with Oil Red O as previously described (17).

Statistical analyses

Statistical analyses (averages, standard deviations, standard errors, Student's *t*-test, Tukey's post hoc test) were performed using JMP version 7.0 (SAS Institute, Cary, NC). Threshold for significance was set at $P \leq 0.05$. For comparison of lipids between WHC heterozygotes and homozygotes, and for comparison of lesion size between WHC and KO, data were log transformed.

Nomenclature and registration of the mutant

This mutation has been registered with Mouse Genome Informatics (MGI; http://www.informatics.jax.org) and has been assigned allele symbol *Ldlr*^{Hlb301}. The MGI accession number is MGI:2683091. The strain is identified in the JAX Mice Database (http://jaxmice.jax.org) as stock number 5061 with the name C57BL/6J-Ldlr<Hlb301>/J.

RESULTS

Identification of the mutant

Four of thirteen G3 mice that shared a common G1 founder had elevated total plasma cholesterol levels compared with B6 controls after consuming the ATH diet for 5 weeks (**Fig. 1**; **Table 2**). Total cholesterol for these four G3 mice was somewhat elevated when mice were fed chow (130%) and were significantly elevated (210%) when they were fed the ATH diet. HDL and triglycerides were unremarkable in the affected G3 animals. The phenotypic deviants were assigned the official name HLB301, with a laboratory nickname of "Wicked High Cholesterol" (WHC), and bred to strain B6 for heritability testing. After ATH diet feeding, 18 of 25 (HLB301 × B6)F1 progeny (10 females

TABLE 3. Plasma lipids in WHC heterozygotes and homozygotes before and after consuming test diets for 5 weeks

Strain	Diet	N (F, M)	Chol F	Chol M	HDL F	HDL M	TG F	TG M
				mg/dl				
WHC$^{+/-}$	C	30, 25	126 (12)	155 (9)[b]	80 (2)	114 (3)[b]	100 (4)	121 (5)[b]
	W	4, 3	190 (17)	233 (14)	117 (11)	185 (14)[b]	68 (3)	89 (11)
	ATH	26, 22	413 (34)	445 (28)	91 (5)	119 (8)[b]	74 (3)	65 (4)
WHC$^{-/-a}$	C	9, 9	248 (13)	278 (18)	116 (3)	172 (19)[b]	140 (12)	201 (24)[b]
	W	4, 8	914 (5)	1,000 (69)	224 (5)	327 (12)[b]	228 (5)	210 (25)
	ATH	7, 10	1,221 (26)	1,444 (118)	567 (57)	469 (23)	692 (149)	786 (111)

WHC, wicked high cholesterol; ENU, mutant strain; $^{+/-}$, heterozygote; $^{-/-}$, homozygote; C, chow diet, age 8 weeks; W, Western diet, age 13 weeks; ATH, atherogenic diet, age 13 weeks; N, number of animals tested per genotpye and diet; F, female; M, male; Chol, total plasma cholesterol; HDL, HDL cholesterol; TG, triglycerides. Values are averages (standard error).

[a] For both sexes and in each diet condition, lipid values in homozygous animals were significantly greater than in heterozygous animals.

[b] Values for males within genotypes and under the same diet condition were significantly greater than female values.

and 8 males) replicated the elevated total plasma cholesterol of 300–500 mg/dl observed in the founders. Further testing indicated additive effects, i.e., homozygous mutant mice showed further exacerbations of total plasma cholesterol after ATH diet feeding, ranging from 1,100 to 2,000 mg/dl (**Table 3**), suggesting that the original G3 founders were heterozygous. This was confirmed when we established a homozygous line and a genotyping assay for the mutation.

Complementation testing

Because the WHC mutant phenotype resembled the phenotype of the *Apoe* and *Ldlr* KO models of hypercholesterolemia, we carried out a complementation test by mating the homozygous WHC mutant to each of these KO strains to observe whether progeny retained the hypercholesterolemia or whether the phenotype was normalized. If the WHC mutation was in either of these genes, progeny would be expected to show an increase in total plasma cholesterol in response to the ATH diet comparable to that of the homozygous KO parent strain because they would carry one mutant allele from WHC and one from the KO. If the WHC mutation was not in these genes, and WHC carried normal *Apoe* or *Ldlr* genes, less of an increase in total cholesterol would be expected, because progeny would harbor only a single copy of the respective mutation causing hypercholesterolemia. Mating WHC to *Apoe* KO showed that this was not the gene, because cholesterol levels in progeny were only in the 300–500 mg/dl range (data not shown). However, progeny from the mating of WHC to *Ldlr* KO showed a response to ATH diet feeding comparable to that of the KO strain, indicating a failure to complement, providing evidence that the WHC mutation resides in the *Ldlr* gene (**Fig. 2**).

Mapping and identification of the mutation

At the same time that the complementation test was being carried out, we mapped WHC by mating it to DBA/2J (D2), a mouse strain that has only a slight increase in plasma lipids when fed the ATH diet (18). Mapping localized the mutation to mouse chromosome 9 at the region containing the obvious candidate *Ldlr*. Sequencing *Ldlr* from WHC revealed a G to A transition mutation at nucleotide 2,096 in exon 14, a region containing six highly conserved cysteine residues (I-VI; **Fig. 3A**). This missense mutation, changing cysteine V at amino acid residue 699 to a tyrosine (C699Y), occurs within the epidermal growth factor precursor homology domain of the protein (Fig. 3B). The WHC mutation abolishes a *Bgl*I restriction site, an observation that facilitated development of a PCR-based assay for identifying heterozygous and homozygous WHC animals (Fig. 3C). Genotyping the original four G3 phenotypic deviants revealed that each was heterozygous for the mutation. This heterozygosity explains our failure to identify the G3 mice as deviant in the baseline lipid measurement (8 weeks of age, consuming chow), because values did not exceed 3.0 standard deviation units from the mean of B6 controls for total plasma cholesterol.

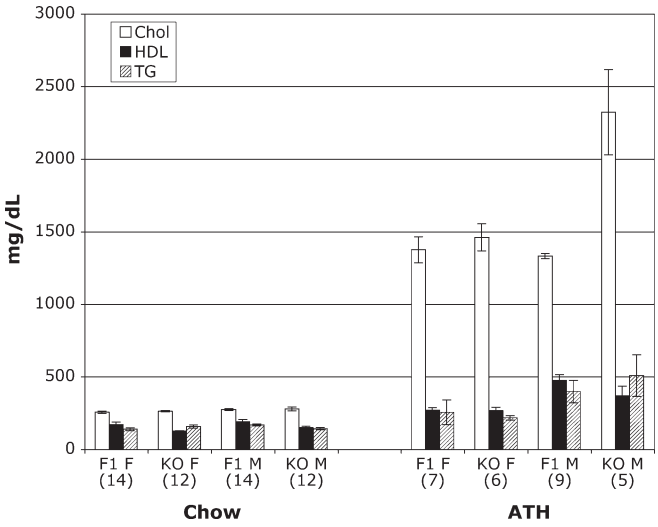

Fig. 2. Complementation testing of wicked high cholesterol (WHC). Homozygous WHC was mated to homozygous LDL receptor (*Ldlr*) knockout (KO) for comparison of lipids in F1 progeny to *Ldlr* KO. F, female; M, male. White bars, total plasma cholesterol; black bars, HDL; stippled bars, triglycerides. Values from animals at 8 weeks of age, consuming chow, are shown on the left half of the graph; values from animals after consuming the ATH diet for 5 weeks (age 13 weeks) are shown on the right half of the graph. The number of animals tested is shown in parentheses below each group. Values are in mg/dl. Error bars are standard error.

Response of WHC to different diets

Heterozygous and homozygous WHC females and males were analyzed for plasma lipids and atherosclerotic lesions after feeding three diets: standard chow, Western diet, or ATH diet. Table 3 shows plasma lipid values for both WHC genotypes in response to consuming these different diets. For both sexes and in each diet condition, all lipid values were greater in homozygous WHC animals than in heterozygotes. However, the following significant sex differences were found among genotypes within the same diet group. In heterozygotes consuming chow, all lipid values were greater in males than in females. In homozygotes consuming chow, males had greater triglyceride and HDL values, whereas total cholesterol did not differ between sexes. On the Western diet, males of each genotype had higher HDL than their female counterparts, whereas other lipid values did not differ. After ATH diet feeding, the only sex difference observed among genotypes was a greater HDL value in heterozygous males than in heterozygous females. Sexes did not differ in total cholesterol or triglycerides among either genotype in response to the ATH diet.

The size of aortic atherosclerotic lesions in WHC mice was influenced by diet and genotype, with some lesions forming in chow-fed mice, larger lesions in Western diet-fed mice, and the largest lesions in ATH diet-fed mice (**Fig. 4**). No difference was observed in lesion size between sexes of WHC for any diet condition or genotype; hence, values for WHC females and males were combined. Lesion area was significantly greater in WHC homozygotes than heterozygotes after Western and ATH diet feeding. Heterozygous WHC animals did not develop lesions on the West-

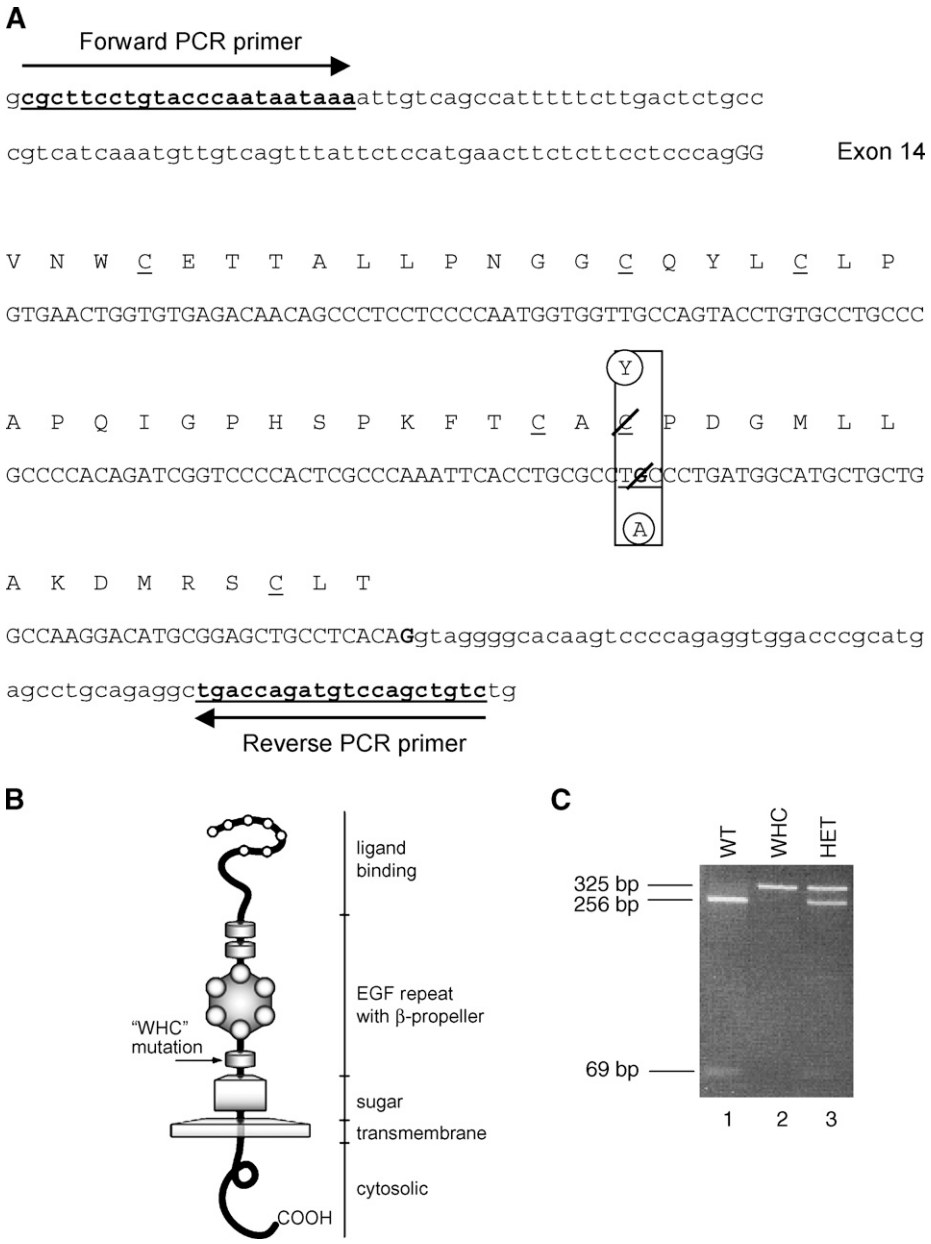

Fig. 3. The WHC mutation. A: Sequence surrounding and including the WHC mutation in exon 14 of the mouse *Ldlr* gene. Boxed area shows the G to A base change at nucleotide 2,096 and change of cysteine to tyrosine at amino acid 699. Nucleotide and amino acid changes due to the mutation are circled. The six highly conserved cysteines (C) within this region of the gene are underlined. Arrows show location and orientation of PCR primer sequences. B: Graphic representation of LDLR molecule showing location of WHC mutation. Functional domains are identified on the right. C: PCR genotyping assay for the WHC mutation includes restriction digest with *Bgl*I. After digestion, WHC homozygotes (lane 2) show a single 325 bp product; WHC heterozygotes (lane 3) show 325, 256, and 69 bp products; wild-type B6 (WT; lane 1) show 256 and 69 bp products.

ern diet, and showed relatively moderate lesions on the ATH diet. No significant difference in lesion area was observed between genotypes in response to chow feeding.

Comparison of WHC homozygotes to *Ldlr* KO strain

Homozygous ($^{-/-}$) WHC mutants and *Ldlr* KO animals were compared for plasma lipids and atherosclerotic lesions after feeding standard chow or the ATH diet. **Figure 5** shows plasma lipid values for females and males of these strains after consuming the different diets. After consuming the chow diet, lipid values for female WHC were not different from those of female KO, nor did male values differ between the strains. In the KO strain, HDL levels were significantly greater in males than in females after chow feeding, as was also observed in WHC. In response to ATH diet feeding, KO animals had significantly higher total plasma cholesterol levels than WHC for both sexes. Additionally, KO males had significantly higher total cho-

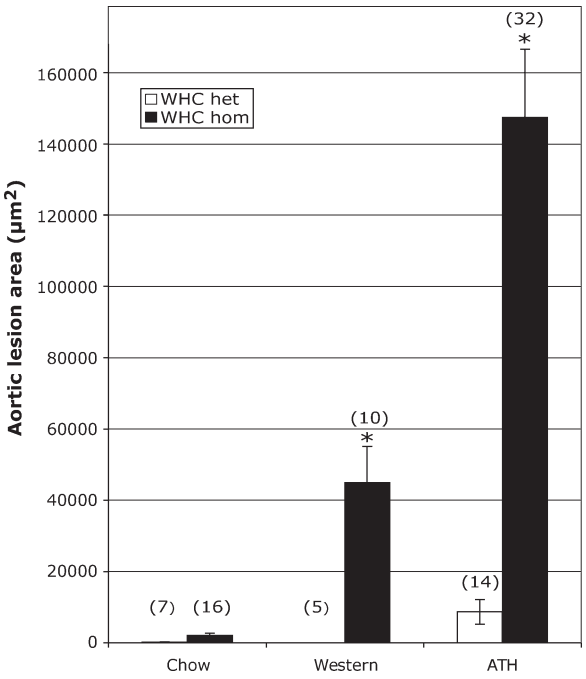

Fig. 4. Atherosclerotic lesion area in WHC heterozygotes and homozygotes. Mice were analyzed under three diet conditions: chow, Western, and ATH. Animals consumed test diets for 5 weeks. Female and male values are combined within each genotype. White bars, WHC heterozygotes; black bars, WHC homozygotes. * Indicates lesions are significantly greater in homozygotes than heterozygotes for the same diet condition. Number of animals tested per genotype for each diet condition is shown in parentheses. Lesion size is expressed in μm^2. Error bars show standard error.

lesterol after ATH diet feeding than KO females, a sex difference not observed in WHC. After ATH diet feeding, HDL and triglycerides, although not significantly different between sexes for either strain, were significantly greater in WHC than in KO animals for both sexes. Therefore, the lipid profile predicts that the KO, with greater total cholesterol and lower HDL, should have larger atherosclerotic lesions than WHC.

Atherosclerotic lesions were significantly larger in WHC mice than *Ldlr* KO after 5 weeks consuming the ATH diet (**Table 4**). As was observed in WHC, no significant difference was found in lesion size between sexes in the KO for any diet condition; hence, lesion sizes shown in Table 4 are combined for KO females and males. In addition to quantitative differences in lesion development in response to the ATH diet, lesions in WHC mice were qualitatively different from lesions in *Ldlr* KO mice (**Fig. 6**). Trichrome staining of aortic lesions in WHC (Fig. 6B) revealed collagen (blue staining) within plaque areas. Early lesions, marked by subendothelial deposition of lipid-laden macrophages, were observed in coronary and pulmonary arteries of WHC mice and not seen in KO mice (Fig. 6C, D).

Histological analysis of livers (**Fig. 7**) suggests that KO mice are prone to earlier fatty changes than WHC when challenged with the ATH diet. The KO mice on the ATH diet (Fig. 7C) had diffuse microvesicular hepatocellular vacuolation that was not observed in B6 (Fig. 7A) or WHC

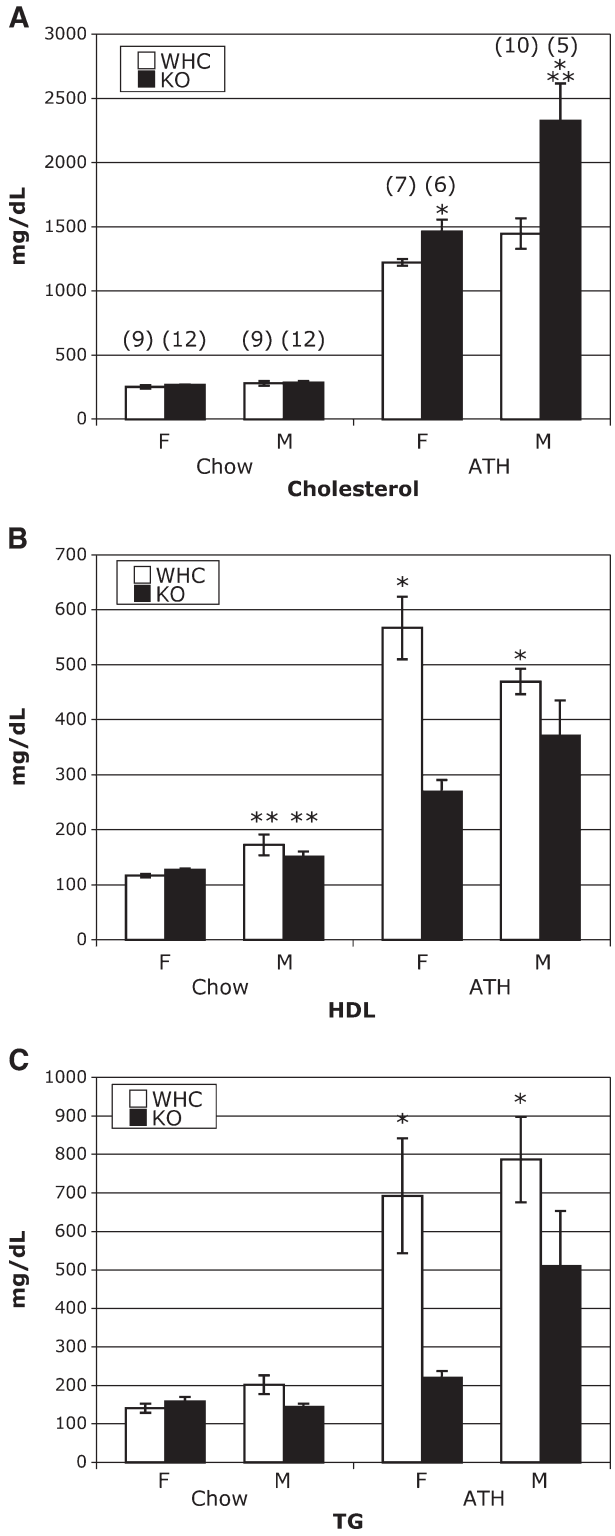

Fig. 5. Comparison of lipids in homozygous WHC and *Ldlr* KO strains before and after consuming the ATH diet for 5 weeks. White bars, WHC; black bars, *Ldlr* KO; F, female; M, male. Chow, standard chow diet, age 8 weeks; ATH, atherogenic fat diet, age 13 weeks. Values are mean ± standard error in mg/dl. A: Total plasma cholesterol; number of animals tested in each group is shown in parentheses and is the same for panels B and C. B: HDL cholesterol. C: Triglycerides. * Indicates significant difference between WHC and KO of same sex under same diet condition ($P \leq 0.05$); ** indicates significant difference between sexes of same strain under same diet condition ($P \leq 0.05$).

TABLE 4. Atherosclerotic lesion area in WHC and *Ldlr* knockout (KO) homozygotes on chow and ATH diets

Strain	N Chow	Chow	N ATH	ATH
		μm^2		μm^2
WHC	16	2,023 (650)	32	147,000 (19,000)[a]
KO	13	116 (67)	11	64,000 (7,000)

Female and male values were combined. N, number of animals tested for the diet condition indicated.

[a] Lesion size in homozygous WHC is significantly greater than in KO after ATH diet feeding.

mice (Fig. 7B) after consuming the ATH diet for the same period of time. Direct staining for lipid to confirm steatosis was not possible on these paraffin-embedded tissues. However, by staining additional KO liver sections with periodic acid-Schiff, we were able to rule out the presence of glycogen in the microvesicles (data not shown).

Additional phenotypic observations in WHC

We bred the WHC mutant to homozygosity and established a line. The WHC strain is viable and fertile in the homozygous state, as is the KO. Two small cohorts of WHC were fed chow or ATH diet until 42 weeks of age. Average lipid levels for each cohort are shown in **Fig. 8A**. Mutant mice fed the ATH diet developed multiple cutaneous xanthomas in the distal limbs, in the skin overlying the mandibular salivary glands (Fig. 8B), and in perineal skin. The skin was often alopecic but there were no epidermal ulcers or excoriations due to pruritis. Histological analysis showed that the dermis was expanded by acicular cholesterol clefts and numerous Langhans-type multinucleated giant cells (Fig. 8C). The renal capsule, mesentery, and other serosal surfaces were diffusely expanded by acicular cholesterol clefts and multinucleated giant cells (Fig. 8D). Coronal sectioning of the brain (Fig. 8E) re-

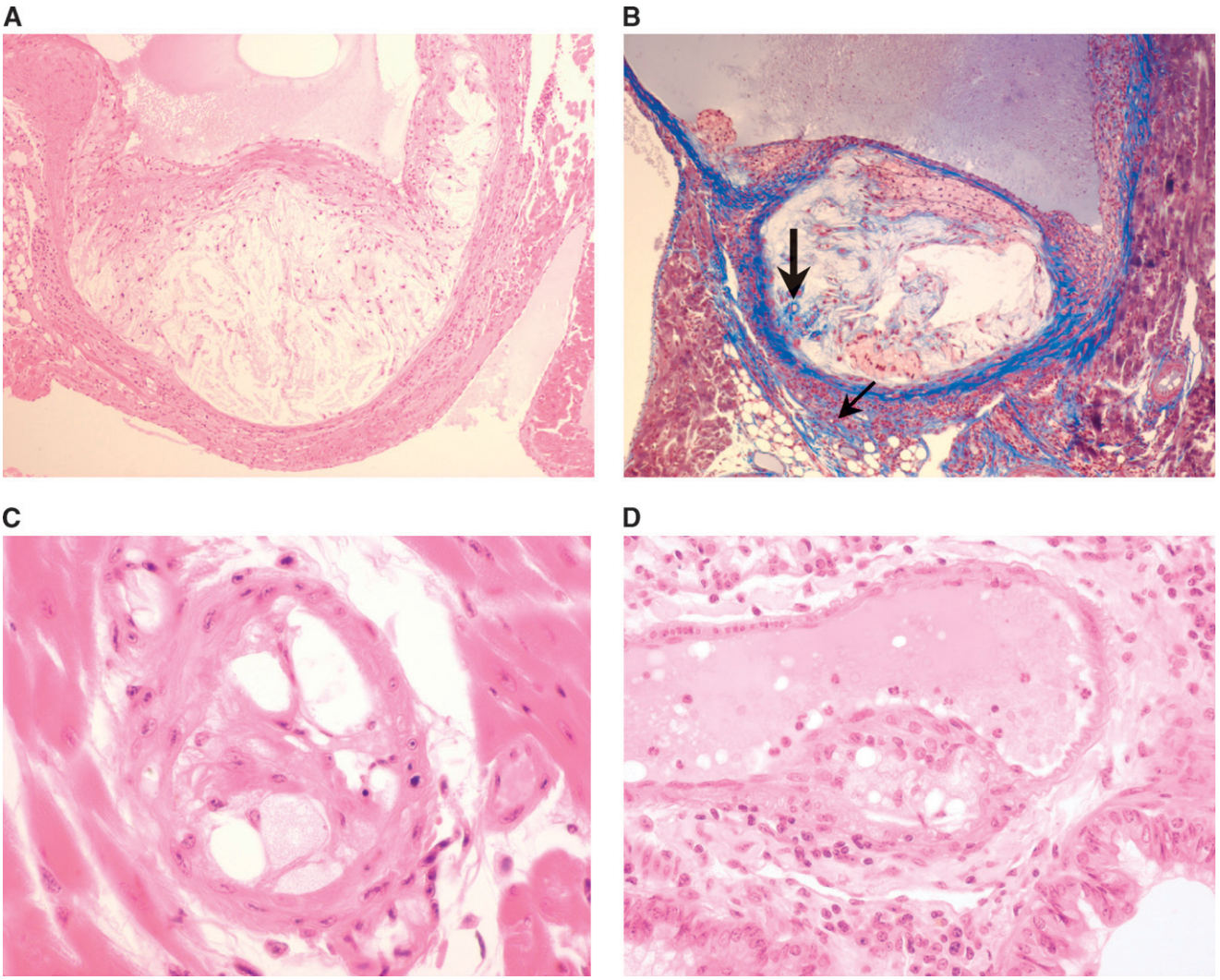

Fig. 6. Histological assessment of atherosclerosis in WHC. A: Hematoxylin and eosin (H and E) staining of aortic valve shows subendothelial accumulation of acicular to poorly defined cholesterol clefts surrounded by a rim of foamy macrophages; 100× magnification. B: Aortic valve stained with Masson's trichrome; 100×. Larger arrow shows subendothelial collagen deposition (blue) within the valve. Smaller arrow shows increased collagen deposition between surrounding cardiac myocytes. C: H and E-stained coronary artery, 600×, shows reduced lumen diameter with almost complete occlusion of the coronary artery owing to subendothelial deposition of foamy macrophages. D: H and E-stained pulmonary artery, 400×, shows accumulation of lipid-loaded macrophages.

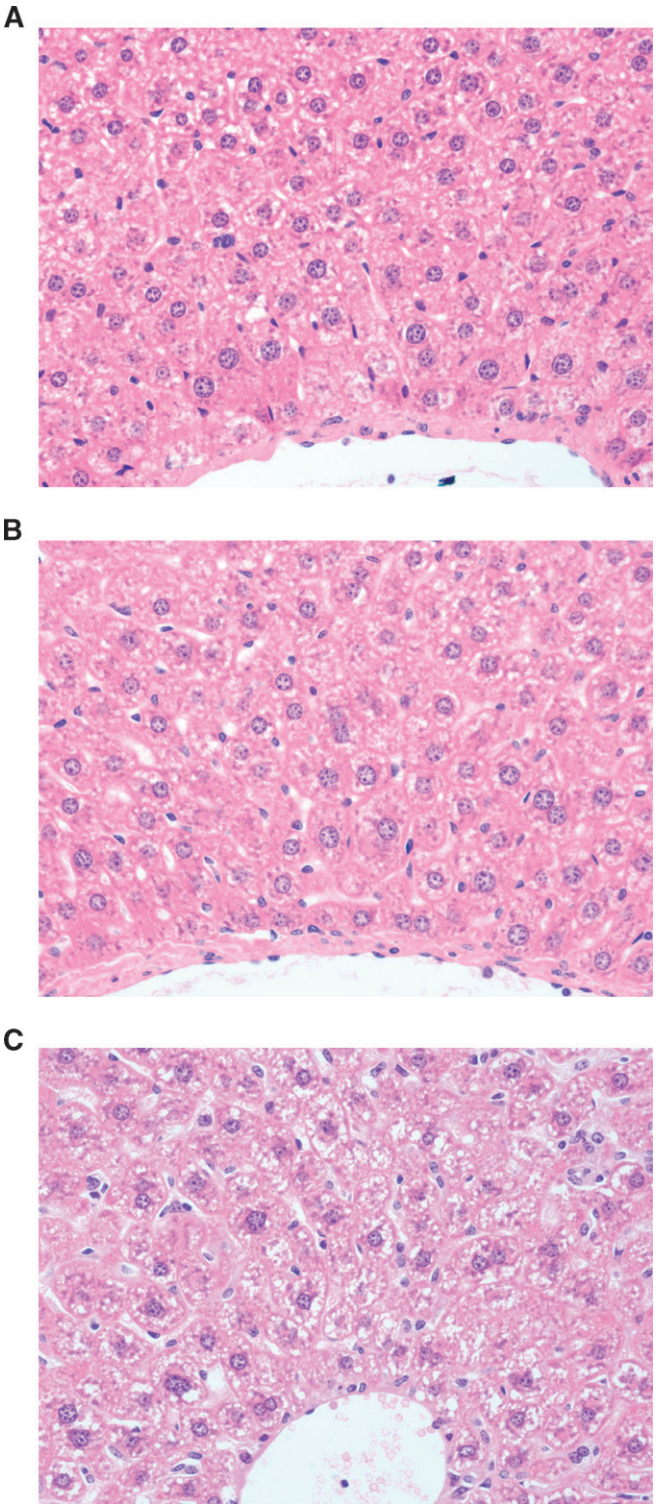

Fig. 7. Fatty liver changes observed in *Ldlr* KO and not in B6 or WHC after 5 weeks of ATH diet feeding. All samples are from 18 week-old males. A: B6. B: WHC homozygote. C: KO homozygote. To standardize comparisons, liver centrolobular vein is shown for each strain. All sections stained with H and E, 400× magnification.

vealed multifocal to coalescing aggregates of foamy macrophages admixed with acicular cholesterol clefts and rare multinucleated giant cells. These aggregates often extended from the choroids plexi in the lateral and third ventricles, and the dense sheets of foamy macrophages effaced and replaced the neural parenchyma (Fig. 8F). Affected animals appeared otherwise normal in gait and home cage behavior. No xanthomas were observed in similarly aged WHC mice fed chow.

DISCUSSION

An important and widely used KO for the mouse *Ldlr* was created 15 years ago (2). In addition to its use as a model of human FH, this strain has been used to develop numerous double mutants, which carry an additional mutation in one of many other key genes involved in atherosclerosis. Using ENU mutagenesis, we have created a new *Ldlr* loss-of-function mutant with phenomic and genomic features that distinguish it from the KO, making it a valuable addition to the current repertoire of hyperlipidemic mouse models.

Differences in phenotype between the KO and ENU *Ldlr* models warrant further investigation into their genomic differences. The KO carries a targeted mutation in exon 4 of the *Ldlr* and produces a truncated receptor, which lacks the membrane-spanning segment and cannot bind LDL. The mutation was created in embryonic stem cells derived from inbred mouse strain 129S7/SvEvBrd (129) and made congenic on background strain B6. Hence, this mouse retains sequences adjacent to the *Ldlr* from the 129 strain. In contrast, the ENU-generated WHC *Ldlr* mouse offers a coisogenic, single-nucleotide *Ldlr* mutation on an otherwise pure B6 genetic background. The genetic differences between these models may account for the phenotypic differences observed in WHC, namely accelerated atherosclerosis and delayed steatosis in response to consuming an ATH diet for a relatively short period. We also observed foam cell accumulation in coronary and pulmonary arteries of WHC mice after the short exposure to the ATH diet, in contrast to other hyperlipidemic models. Even though total plasma cholesterol was lower and HDL cholesterol and triglycerides were higher in WHC compared with *Ldlr* KO after ATH diet feeding, advanced lesion formation persisted in WHC. Furthermore, lesion size in WHC homozygous mice fed the Western diet was the same as KO mice fed the ATH diet. Differences described in this report between the ENU mutant and the KO in response to the ATH diet may be attributable to residual 129 sequences in the *Ldlr* KO harboring a "passenger gene" effect (19). Restriction-fragment-length variation within the *Ldlr* gene between different inbred mouse strains has also been described. However, strains 129 and B6 share a common restriction-fragment length polymorphism haplotype for *Ldlr* (20).

We localized the WHC mutation to exon 14 of the *Ldlr*, within the EGF precursor repeat domain. Hobbs et al. (21) have described mutations in this domain as class 2 LDLR mutations, which are transport defects resulting in complete loss of receptor function, and comprise the most common human FH mutations. We therefore predict that

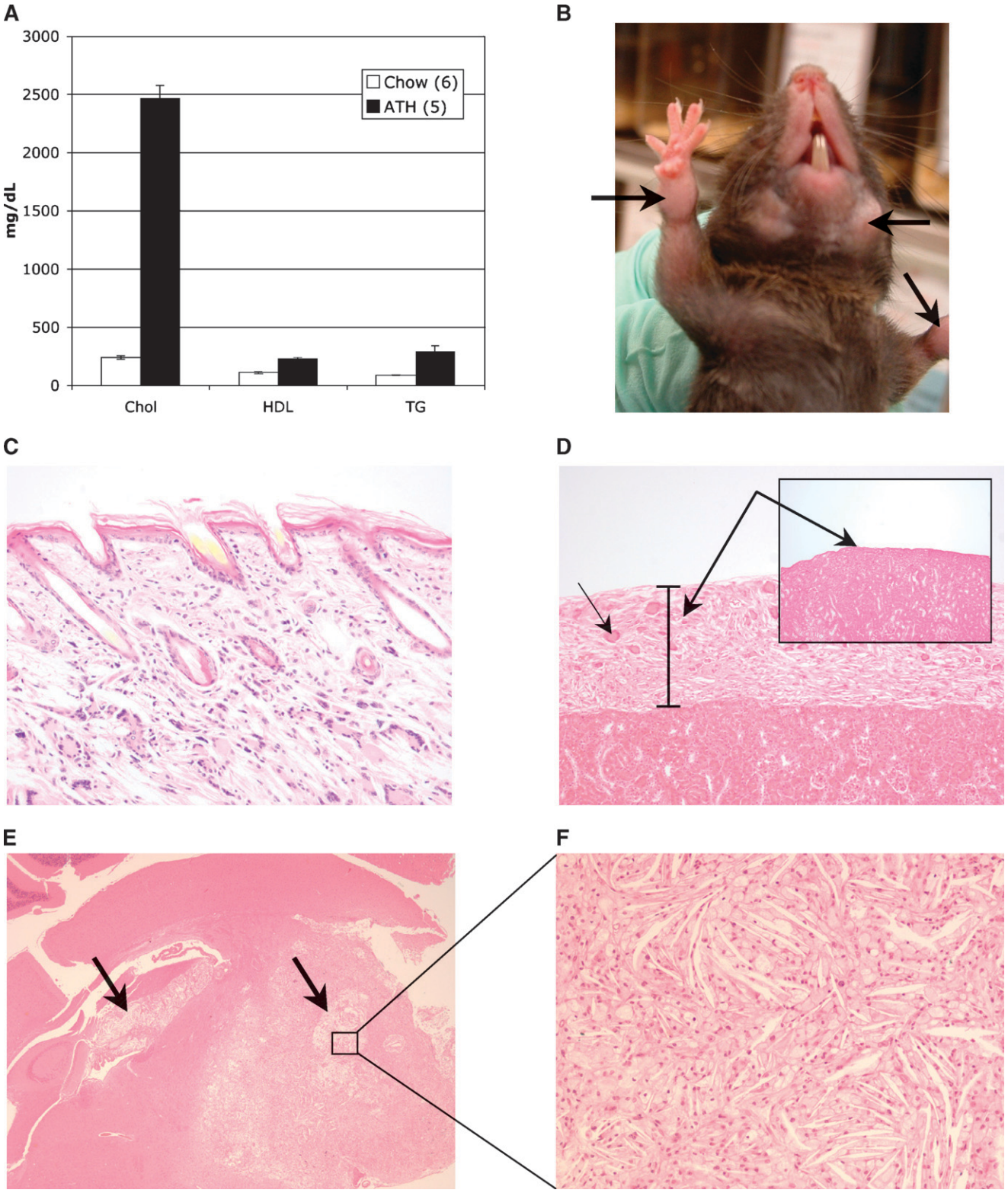

Fig. 8. Phenotypes of 42 week-old homozygous WHC mice. A: Average lipid levels after being maintained on chow (white bars; n = 6) or after ATH diet feeding for 34 weeks (black bars; n = 5). Female and male values were not significantly different and were combined for each diet condition. B: ATH-fed WHC mouse, age 42 weeks. Arrows indicate cutaneus xanthomas in distal forelimbs and skin overlying mandibular salivary glands. C: Skin section from forelimb xanthoma showing cholesterol cleft accumulation; H and E stain, 200× magnification. D: Kidney, H and E-stained, 200×. Bar defines renal capsule expanded by cholesterol clefts and Langhans-type multinucleated giant cells (small arrow). Inset shows age-matched B6 control kidney, H and E stain. E: Brain, coronal section at the hippocampal level; left arrow points to hippocampus and shows large coalescing areas of encephalomalacia and partial effacement of the hippocampus and the thalamic nuclei; right arrow points to putamen and globus pallidus nuclei, showing extensive loss of brain parenchyma and replacement by acicular cholesterol clefts and dense sheets of foamy macrophages; lesion extends into thalamic nuclei; H and E stain, 20×. F: Enlargement of boxed area in E; H and E stain, 200×.

the WHC mutation causes improper folding of the receptor, resulting in failure of the protein to be transported from the endoplasmic reticulum to the Golgi for processing to the cell surface. In humans, the comparable WHC mutation (C677Y), also a G to A transition at conserved cysteine V, rare among exon 14 mutations, has been reported in three patients with familial hypercholesterolemia (FH) (22–24). In an analysis of human *Ldlr* mutations by Salazar and colleagues (23), missense mutations were associated with higher HDL levels in heterozygous FH patients than frameshift or nonsense mutations. We observed higher HDL in the missense mutant WHC mice than in the *Ldlr* KO mice. It is notable when comparing the mouse with human FH phenotypes that, in general, patients heterozygous for *Ldlr* mutations present severe phenotypes as a result of hyperlipidemia, whereas WHC and *Ldlr* KO mice require homozygosity to more closely mimic the human disease.

High-throughput phenotyping of mouse ENU mutants has revealed novel, single-base mutations in disease-related genes and produced numerous robust models of human disorders (25–32). These ENU mutants are otherwise genetically identical to their nonmutagenized inbred strain counterparts, allowing highly specific analyses of the functional consequence of a single base change, and often produce distinctly different phenotypes from those observed in analogous KO models. This collection of mutants allows important refinement of gene function and biological pathways, leading to better models of human disease.

The authors thank Cynthia McFarland for quantitative analysis of atherosclerotic lesions, Roderick Bronson for evaluation of histologic specimens, and Weidong Zhang for help with statistical analyses. The Jackson Laboratory Scientific Services department provided assistance in genetic mapping, histology, and graphic services.

REFERENCES

1. Piedrahita, J. A., S. H. Zhang, J. R. Hagaman, P. M. Oliver, and N. Maeda. 1992. Generation of mice carrying a mutant apolipoprotein E gene inactivated by gene targeting in embryonic stem cells. *Proc. Natl. Acad. Sci. USA*. **89:** 4471–4475.
2. Ishibashi, S., M. S. Brown, J. L. Goldstein, R. D. Gerard, R. E. Hammer, and J. Herz. 1993. Hypercholesterolemia in low density lipoprotein receptor knockout mice and its reversal by adenovirus-mediated gene delivery. *J. Clin. Invest.* **92:** 883–893.
3. Warden, C. H., C. C. Hedrick, J. H. Qiao, L. W. Castellani, and A. J. Lusis. 1993. Atherosclerosis in transgenic mice overexpressing apolipoprotein A-II. *Science*. **261:** 469–472.
4. Farese, R. V., Jr., M. M. Veniant, C. M. Cham, L. M. Flynn, V. Pierotti, J. F. Loring, M. Traber, S. Ruland, R. S. Stokowski, D. Huszar, et al. 1996. Phenotypic analysis of mice expressing exclusively apolipoprotein B48 or apolipoprotein B100. *Proc. Natl. Acad. Sci. USA*. **93:** 6393–6398.
5. Leppanen, P., J. S. Luoma, M. H. Hofker, L. M. Havekes, and S. Yla-Herttuala. 1998. Characterization of atherosclerotic lesions in apo E3-leiden transgenic mice. *Atherosclerosis*. **136:** 147–152.
6. Miyake, J. H., X. T. Duong-Polk, J. M. Taylor, E. Z. Du, L. W. Castellani, A. J. Lusis, and R. A. Davis. 2002. Transgenic expression of cholesterol-7-alpha-hydroxylase prevents atherosclerosis in C57BL/6J mice. *Arterioscler. Thromb. Vasc. Biol.* **22:** 121–126.
7. Hardisty, R. E., A. Erven, K. Logan, S. Morse, S. Guionaud, S. Sancho-Oliver, A. J. Hunter, S. D. Brown, and K. P. Steel. 2003. The deaf mouse mutant Jeff (Jf) is a single gene model of otitis media. *J. Assoc. Res. Otolaryngol.* **4:** 130–138.
8. Ahituv, N., A. Erven, H. Fuchs, K. Guy, R. Ashery-Padan, T. Williams, M. H. de Angelis, K. B. Avraham, and K. P. Steel. 2004. An ENU-induced mutation in AP-2alpha leads to middle ear and ocular defects in Doarad mice. *Mamm. Genome*. **15:** 424–432.
9. Toye, A. A., L. Moir, A. Hugill, L. Bentley, J. Quarterman, V. Mijat, T. Hough, M. Goldsworthy, A. Haynes, A. J. Hunter, et al. 2004. A new mouse model of type 2 diabetes, produced by N-ethyl-nitrosourea mutagenesis, is the result of a missense mutation in the glucokinase gene. *Diabetes*. **53:** 1577–1583.
10. Yu, Q., Y. Shen, B. Chatterjee, B. H. Siegfried, L. Leatherbury, J. Rosenthal, J. F. Lucas, A. Wessels, C. F. Spurney, Y. J. Wu, et al. 2004. ENU induced mutations causing congenital cardiovascular anomalies. *Development*. **131:** 6211–6223.
11. Feng, J., H. Wang, and H. C. Morse III. 2007. Functional deficiency in IL-7 caused by an N-ethyl-N-nitrosourea-induced point mutation. *Genetics*. **175:** 545–551.
12. Svenson, K. L., M. A. Bogue, and L. L. Peters. 2003. Identifying new mouse models of cardiovascular disease: a review of high-throughput screens of mutagenized and inbred strains. *J. Appl. Physiol.* **94:** 1650–1659.
13. Justice, M. J., D. A. Carpenter, J. Favor, A. Neuhauser-Klaus, M. Hrabe de Angelis, D. Soewarto, A. Moser, S. Cordes, D. Miller, V. Chapman, et al. 2000. Effects of ENU dosage on mouse strains. *Mamm. Genome*. **11:** 484–488.
14. Weber, J. S., A. Salinger, and M. J. Justice. 2000. Optimal N-ethyl-N-nitrosourea (ENU) doses for inbred mouse strains. *Genesis*. **26:** 230–233.
15. Nishina, P., J. Wang, W. Toyofuku, F. Kuypers, B. Ishida, and B. Paigen. 1993. Atherosclerosis and plasma and liver lipids in nine inbred strains of mice. *Lipids*. **28:** 599–605.
16. Taylor, B. A., and S. J. Phillips. 1996. Detection of obesity QTLs on mouse chromosomes 1 and 7 by selective DNA pooling. *Genomics*. **34:** 389–398.
17. Paigen, B., A. Morrow, P. A. Holmes, D. Mitchell, and R. A. Williams. 1987. Quantitative assessment of atherosclerotic lesions in mice. *Atherosclerosis*. **68:** 231–240.
18. Svenson, K. L., R. Von Smith, P. A. Magnani, H. R. Suetin, B. Paigen, J. K. Naggert, R. Li, G. A. Churchill, and L. L. Peters. 2007. Multiple trait measurements in 43 inbred mouse strains capture the phenotypic diversity characteristic of human populations. *J. Appl. Physiol.* **102:** 2369–2378.
19. Lusis, A. J., J. Yu, and S. S. Wang. 2007. The problem of passenger genes in transgenic mice. *Arterioscler. Thromb. Vasc. Biol.* **27:** 2100–2103.
20. Srivastava, R. A., B. A. Pfleger, and G. Schonfeld. 1991. Expression of LDL receptor, apolipoprotein B, apolipoprotein A-I and apolipoprotein A-IV mRNA in various mouse organs as determined by a novel RNA-excess solution hybridization assay. *Biochim. Biophys. Acta*. **1090:** 95–101.
21. Hobbs, H. H., D. W. Russell, M. S. Brown, and J. L. Goldstein. 1990. The LDL receptor locus in familial hypercholesterolemia: mutational analysis of a membrane protein. *Annu. Rev. Genet.* **24:** 133–170.
22. Schmidt, H., and G. M. Kostner. 2000. Familial hypercholesterolemia in Austria reflects the multi-ethnic origin of our country. *Atherosclerosis*. **148:** 431–432.
23. Salazar, L. A., M. H. Hirata, S. A. Cavalli, E. R. Nakandakare, N. Forti, J. Diament, S. D. Giannini, M. C. Bertolami, and R. D. Hirata. 2002. Molecular basis of familial hypercholesterolemia in Brazil: identification of seven novel LDLR gene mutations. *Hum. Mutat.* **19:** 462–463.
24. Mozas, P., S. Castillo, D. Tejedor, G. Reyes, R. Alonso, M. Franco, P. Saenz, F. Fuentes, F. Almagro, P. Mata, et al. 2004. Molecular characterization of familial hypercholesterolemia in Spain: identification of 39 novel and 77 recurrent mutations in LDLR. *Hum. Mutat.* **24:** 187.
25. Vitaterna, M. H., D. P. King, A. M. Chang, J. M. Kornhauser, P. L. Lowrey, J. D. McDonald, W. F. Dove, L. H. Pinto, F. W. Turek, and J. S. Takahashi. 1994. Mutagenesis and mapping of

a mouse gene, Clock, essential for circadian behavior. *Science.* **264:** 719–725.
26. Inoue, M., Y. Sakuraba, H. Motegi, N. Kubota, H. Toki, J. Matsui, Y. Toyoda, I. Miwa, Y. Terauchi, T. Kadowaki, et al. 2004. A series of maturity onset diabetes of the young, type 2 (MODY2) mouse models generated by a large-scale ENU mutagenesis program. *Hum. Mol. Genet.* **13:** 1147–1157.
27. Mohr, M., M. Klempt, B. Rathkolb, M. H. de Angelis, E. Wolf, and B. Aigner. 2004. Hypercholesterolemia in ENU-induced mouse mutants. *J. Lipid Res.* **45:** 2132–2137.
28. Kermany, M. H., L. L. Parker, Y. K. Guo, D. Miller, D. J. Swanson, T. J. Yoo, D. Goldowitz, and J. Zuo. 2006. Identification of 17 hearing impaired mouse strains in the TMGC ENU-mutagenesis screen. *Hear. Res.* **220:** 76–86.
29. Keays, D. A., G. Tian, K. Poirier, G. J. Huang, C. Siebold, J. Cleak, P. L. Oliver, M. Fray, R. J. Harvey, Z. Molnar, et al. 2007. Mutations in alpha-tubulin cause abnormal neuronal migration in mice and lissencephaly in humans. *Cell.* **128:** 45–57.
30. Cook, M. N., J. P. Dunning, R. G. Wiley, E. J. Chesler, D. K. Johnson, D. R. Miller, and D. Goldowitz. 2007. Neurobehavioral mutants identified in an ENU-mutagenesis project. *Mamm. Genome.* **18:** 559–572.
31. Davies, V. J., K. A. Powell, K. E. White, W. Yip, V. Hogan, A. J. Hollins, J. R. Davies, M. Piechota, D. G. Brownstein, S. J. Moat, et al. 2008. A missense mutation in the murine Opa3 gene models human Costeff syndrome. *Brain.* **131:** 368–380.
32. Aigner, B., B. Rathkolb, N. Herbach, M. Hrabe de Angelis, R. Wanke, and E. Wolf. 2008. Diabetes models by screen for hyperglycemia in phenotype-driven ENU mouse mutagenesis projects. *Am. J. Physiol. Endocrinol. Metab.* **294:** E232–E240.